

# HYBRID COMPOSITE LAMINATES FOR HIGH-PERFORMANCE BOLTED JOINTS

Pedro P. Camanho <sup>1</sup>, Axel Fink <sup>2</sup>, Soraia Pimenta <sup>1</sup>, Andreas Obst <sup>3</sup>

<sup>1</sup>DEMEGI, Faculdade de Engenharia, Universidade do Porto  
Rua Dr. Roberto Frias, 4200-465 Porto, Portugal

<sup>2</sup>DLR German Aerospace Center – Inst. of Composite Structures & Adaptive Systems  
Lilienthalplatz 7, D-38108 Braunschweig, Germany

<sup>3</sup>ESA-ESTEC, Mechanical Engineering Dept.  
Keplerlaan 1, NL-2200 AG Noordwijk, The Netherlands

## ABSTRACT

This paper presents a numerical investigation of the mechanical response of new hybrid composite laminates based on the substitution of CFRP plies with titanium plies. This technology is proposed for bolted joints that are very often the critical part of composite structures. Two modelling strategies, one applicable to the bolt-bearing region and another to the transition region of the hybrid laminate, are proposed. The numerical results indicate that the use of hybrid composites can drastically increase the strength of CFRP bolted joints and therefore increase the efficiency of this type of joint.

## 1. INTRODUCTION

One of the main methods used for joining composite components for aircraft and spacecraft applications is mechanical fastening [1]. Mechanically fastened joints have the advantages of reliability, detachability and inspectability, and represent a well-established and well-known method. However, to reach a satisfactory structural coupling efficiency with composite materials is much more challenging than it is for metals due to the low bearing and shear strengths, the higher notch sensitivity, the dependence of the joint strength on laminate configuration, and the influence of environmental effects. These properties represent a limiting factor on the structural performance of composite structures.

The load capacity of composite bolted joints is typically increased by means of a local laminate build-up at the structure coupling area. The resulting laminate thickness increase leads to additional laminate stresses due to eccentricities, particularly in the case of single-shear joints, to complex geometries of adjacent structures as well as to a significant weight increase due to larger grip lengths, larger bolt diameters and heavier metallic fittings. The increasing requirements for weight reduction and cost efficiency for aerospace and spacecraft structures demand the development of alternative advanced coupling techniques.

The coupling efficiency of highly loaded composite joints has been proven, in the frame of extensive previous research activities at the German Aerospace Centre [1-3], to be considerably improved by the use of a local reinforcement of the joining area with thin high-strength metal foils using ply substitution techniques. The use of a hybrid composite increases the bearing strength, the coupling stiffness and reduces the sensitivity of the mechanical properties to the laminate configuration and environmental effects. Higher absolute mechanical properties prevent any local laminate thickening and eccentricities and allow possible reductions of the number of bolts and bolt rows, resulting in a mechanically and cost efficient design.

The objective of this paper is to present the numerical analysis of the inelastic response of hybrid carbon-epoxy/titanium bolted joints. The numerical studies are focused on the mechanical performance improvement in comparison to the reference conventional design. The delamination behaviour of the transition region, which is characterized by a gradual replacement of certain composite plies, is analyzed by means of numerical simulations. The simulation of the bolt bearing region is performed using a model that accounts for ply failure mechanisms, combined with a plasticity model that simulates the mechanical response of the titanium inserts.

## 2. HYBRID COMPOSITES BASED ON PLY SUBSTITUTION

The local reinforcement technique applied to the bolt-bearing region is accomplished by the gradual substitution of specific composite plies by high-strength metal foils within the coupling region (Fig. 1). The remaining composite plies are not interrupted and pass from the pure composite region through the transition region to the hybrid region, thus acting there as adhesion interlayers between each embedded metal foil. The continuous plies should preferably contribute most to the total load carrying of the laminate.

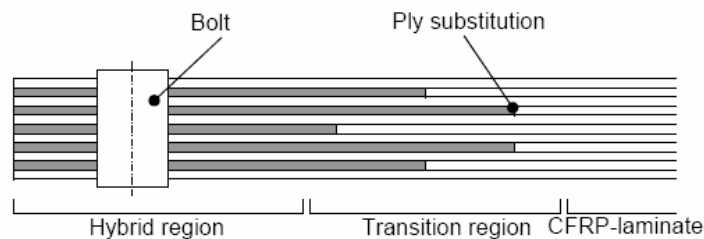


Figure 1: Hybrid composite at the bolted joint location.

Figure 2 a) and b) show respectively the through-the-thickness cross-sections of the bolt-bearing region and of the transition region.

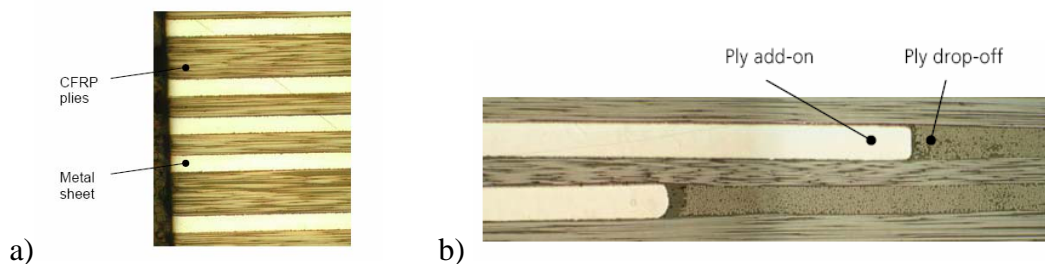


Figure 2: Details of the a) bolt-bearing and b) transition regions.

The selection of the metal to be used in the locally reinforced region of the laminate is of primary importance to the efficiency of the technology proposed. Taking into account that titanium has good specific mechanical properties, is electrochemically compatible with carbon, and has a relatively low coefficient of thermal expansion, this material is selected for the metal layers.

The hybrid composite material can be manufactured using different technologies such as pre-preg lay-up, resin infusion and fibre placement. All these techniques were

successfully demonstrated in previous investigations [1-3]. When using the pre-preg technique, the lay-up process consists of stacking alternate layers of titanium alloy foils (Ti6Al4V or Ti15-3-3-3) and pre-preg plies without adding any adhesive. The selected titanium surface pre-treatment consists of a surface cleaning and a chemical pickling pre-treatment which provides an optimal adhesion quality between the metal and the pre-preg resin. Higher adhesion performance and delamination growth attenuation is achieved generating a metal surface macro-roughness by means of surface grit blasting. Previous experimental analyses [1] have demonstrated that the use of hybrid laminates with 20% titanium content increases the tensile strength of a three-row bolted joint by 91% when compared to that of a full CFRP laminate, whereas the specific tensile strength is increased by 32%. This means that the joint based on the hybrid composite is lighter and it does not require a local increase of the thickness that would trigger secondary bending effects in single-shear joints and increase bolt bending. Therefore, the weight gains in actual composite structures may be even higher than the values obtained by comparing the specific joint strength of test coupons.

Based on the promising experimental results obtained in [1-3], it is necessary to define a methodology to design hybrid composites. The design methodology proposed here is based on the use of computational models that predict the onset and propagation of the failure mechanisms that occur at the bolt bearing and transition regions.

### **3. NUMERICAL ANALYSIS OF HYBRID COMPOSITES**

#### **3.1 Bolt-bearing region**

##### **3.1.1 Model definition**

The use of a fully three-dimensional (3D) finite element model is recommended for the failure analyses of composite bolted joints [4]. The need for a fully 3D model is justified by the relevance of the out-of-plane components of the stress tensor in the failure mechanisms, by the possible existence of delamination in joints where no clamping pressure is applied, and by the need to accurately compute the contact tractions between the bolt and the laminate.

Abaqus [5] finite element code is used for the analyses. The progressive damage model implemented in Abaqus uses of the Hashin's failure criteria [6] for the prediction of the onset of the different types of intralaminar damage that occur in laminated composites: fibre tensile fracture, fibre kinking, matrix tensile cracking and matrix compressive failure. In addition, the damage model predicts the accumulation and propagation of the different ply damage mechanisms. This is accomplished by defining a linear damage evolution law that is based on the material toughness for each failure mechanism. Although this procedure ensures that the computed energy dissipation is independent of the mesh refinement, it should be noted that previous investigations of the authors [7]-[8] have shown that for failure modes that include several energy dissipation mechanisms (such as tensile failure in the longitudinal direction that involves fibre failure, fibre-matrix pull out and matrix cracking) a bi-linear cohesive law is more appropriate.

Abaqus [5] progressive damage model is defined using plane stress conditions, so it requires the use of elements in a plane stress state. Therefore, the composite layers were modelled using 3D linear hexahedral elements with a plane stress formulation ("continuum shell" elements, referenced as SC8R), with reduced integration and hourglass control. M40/CYCOM 977-2 carbon epoxy unidirectional plies with a nominal ply thickness of 0.25mm are used in the simulation. The CFRP material

properties (elastic and strength) required for the analyses are presented in the following tables:

$E_1$ (MPa)	$E_2$ (MPa)	$G_{12}$ (MPa)	$G_{13}$ (MPa)	$\nu_{12}$	$\nu_{23}$
211424	6287	3895	2096	0.3	0.5

Table 1: Ply elastic properties.

$X_T$ (MPa)	$X_C$ (MPa)	$Y_T$ (MPa)	$Y_C$ (MPa)*	$S_L$ (MPa)*
1665	994	47	217	67

\*values measured in unidirectional specimens

Table 2: Ply strengths.

The coefficients of thermal expansion of M40/CYCOM 977-2 are  $\alpha_{11} = -0.84 \times 10^{-6}/^\circ\text{C}$  and  $\alpha_{22} = 29.1 \times 10^{-6}/^\circ\text{C}$ . Additionally, the damage models used in the simulations require the in-situ strengths and fracture toughness. The values fracture energies measured at NASA-Langley for IM7/977-2 carbon epoxy,  $G_{Ic} = 0.306\text{N/mm}$  (delamination in mode I or matrix tension),  $G_{IIc} = 1.680\text{N/mm}$  (delamination in mode II), and at the University of Porto [6],  $G_{1+} = 81.5\text{N/mm}$  (fibre tension),  $G_{1-} = 106.3\text{N/mm}$  (fibre compression). With these values, it is possible to calculate also the matrix compression fracture energy as  $G_{2-} = 7.48\text{N/mm}$ , and the in-situ shear and transverse tensile strengths as presented in Table 3.

Ply	$Y_T$ (MPa)	$S_L$ (MPa)
Outer	62.6	102.1
Inner	99.0	124.8

Table 3: Ply in-situ strengths.

An elasto-plastic material model is selected for the titanium used in the hybrid composite and in the bolt. The Von Mises criterion is used to predict the onset of plastic flow. The plastic deformation is defined by an isotropic hardening behaviour, and by an associated flow rule where the inelastic deformation rate is in the direction of the normal of the yield surface. The coefficient of thermal expansion of the titanium is  $\alpha = 9.2 \times 10^{-6}/^\circ\text{C}$ . The mechanical properties of the titanium are presented in Table 4.

$E$ (GPa)	$\sigma_{0.2\%}$ (MPa)	$\sigma_r$ (MPa)
116	1534	1634

Table 4: Properties of the Ti15-3-3-3 titanium layer.

The specimen was meshed using two different approaches. In the neighbourhood of the hole, where damage takes place, a refined mesh was used, using small elements with dimensions of  $0.25\text{mm} \times 0.25\text{mm} \times 0.25\text{mm}$ ; the elements composing this mesh are continuum shell elements, with the damage model implemented for the CFRP plies.

The coarse mesh, approximately four times less refined, is connected to the fine mesh by a surface-to-surface based TIE constraint [5], which allows the correct simulation of the stress distribution at the interface between the two meshes. As before, continuum shell elements were also used, but implementing a linear elastic orthotropic behaviour, as damage is not expected to occur in the region away from the hole.

The bolt is modelled by a simple cylinder made of titanium, meshed with fully-integrated 3D linear hexahedral elements. The mesh of the bolt is twice less refined than that of the composite.

For all specimens, the mid-plane symmetry of the laminate (plane 1-2 in Figure 3) was taken into account, by applying proper boundary conditions. Whenever possible (absence of  $\pm 45$  plies), a symmetry with respect to the plane 1-3 shown in Figure 3 was also considered to reduce the computation time.

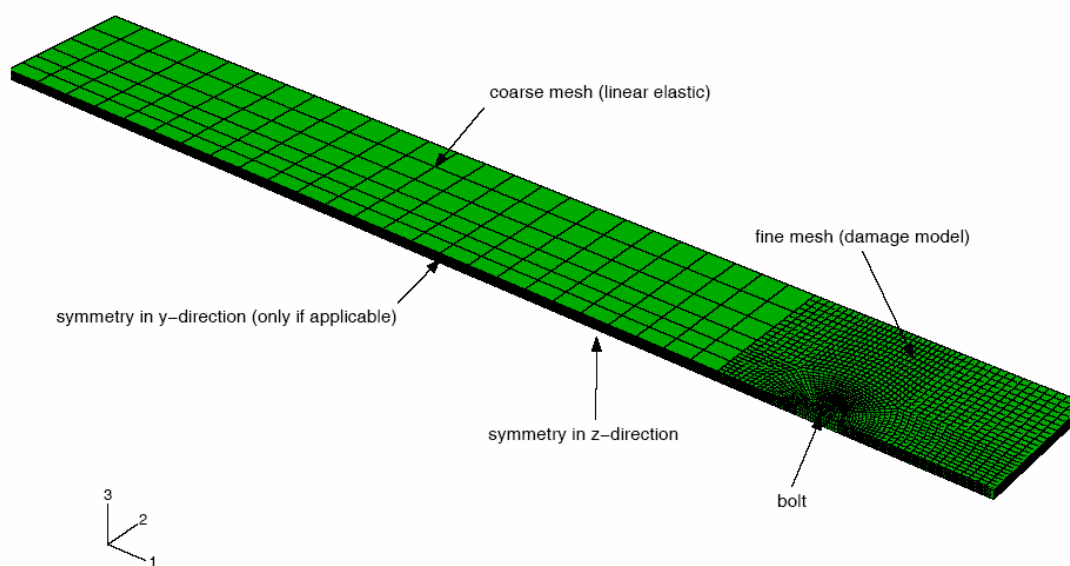


Figure 3: Finite element mesh.

An initial thermal step with  $\Delta T = -155^\circ\text{C}$  was applied to the test specimen to simulate the curing process (from  $T = 180^\circ\text{C}$  to  $T = 25^\circ\text{C}$ ). During this step, the laminate was allowed to contract freely, and the bolt (without thermal load applied) was centred within the hole by specifying kinematic constraints. An intermediate step, corresponding to the attachment of the specimen to the test machine, is applied afterwards.

Finally, the bearing test is simulated: a constant velocity along the 1-axis shown in Figure 3 is imposed to the bolt's axis and top surface, and additionally proper kinematic conditions are imposed in order to ensure the correct alignment of the parts.

The kinematic constraint between the bolt and the specimen's hole is removed, and a contact definition is activated to allow the surface of the bolt to drag the surface of the hole during the test. Friction between the bolt and the laminate is taken into account in the analyses. The contact is assumed to follow Coulomb's friction law and a coefficient of friction between the bolt and the laminate of 0.3 is used [10].

### 3.2.2 Numerical results

Three different laminates are simulated: one baseline configuration corresponding to an all CFRP bolted joint, and three hybrid composites as shown in Table 5. All laminates are 45mm wide, 170mm long, and have a 6.35mm diameter hole. The distance between the centre of the hole and the end of the specimen (end distance) is 25mm.

Reference	Lay-up
B1	[0/45/0/90/-45/0] <sub>s</sub>
B6	[0/45/0/Ti/-45/0] <sub>s</sub>
B7	[0/Ti/0/90/Ti/0] <sub>s</sub>
B8	[0/Ti/0/Ti/0/Ti/0 <sub>1/2</sub> ] <sub>s</sub>

Table 5: Lay-ups simulated.

The comparison between the different material systems used is based on the predicted maximum bearing stress sustained by the joint. The bearing stress,  $\sigma^b$ , is defined as:

$$\sigma^b = \frac{P}{dt} \quad (1)$$

where  $P$  is the applied load,  $t$  is the specimen thickness and  $d$  is the hole diameter. Table 6 shows the predicted bearing strengths,  $\bar{\sigma}^b$ , and remote strength,  $\bar{\sigma}^\infty = P/(wt)$  where  $w$  is the specimen width, for the different specimens simulated. Bearing failure is predicted for all the specimens simulated.

Reference	$\bar{\sigma}^b$ (MPa)	$\bar{\sigma}^\infty$ (MPa)
B1	540.8	76.0
B6	838.7	118.3
B7	1115.2	157.4
B8	1397.0	197.0

Table 6: Predicted failure stresses.

Figure 4 shows the predicted relation between the bearing stress and the bolt displacement for all specimens simulated.

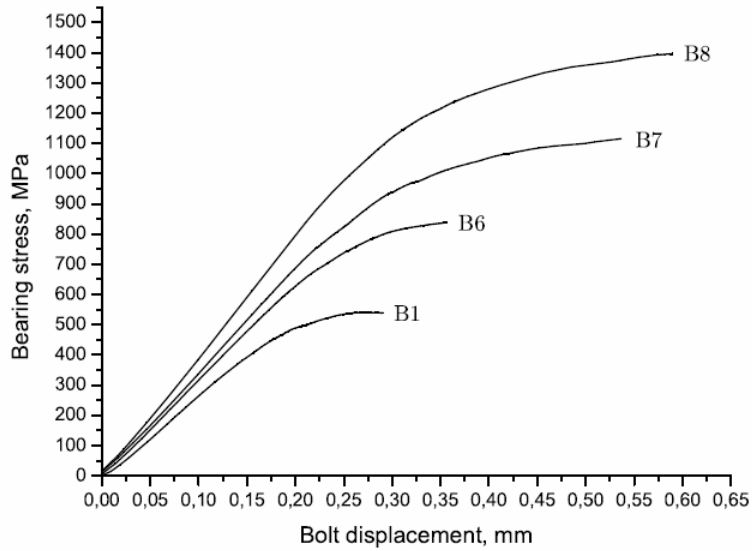


Figure 4: Predicted load-displacement relation.

### 3.2 Transition region

#### 3.2.1 Model definition

The numerical analysis of the test specimens of the transition region is performed by modelling the free-edge of the laminate along the longitudinal direction assuming a two-dimensional plane stress state. This solution is proposed because in the actual specimens delamination is triggered by the singular stress distribution that occurs in the free-edge of the laminate, which is the region where failure initiation takes place. The geometries of the transition region simulated are shown in Figures 5-7.

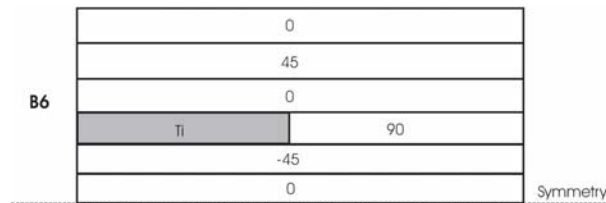


Figure 5: Geometry of the B6 specimen.

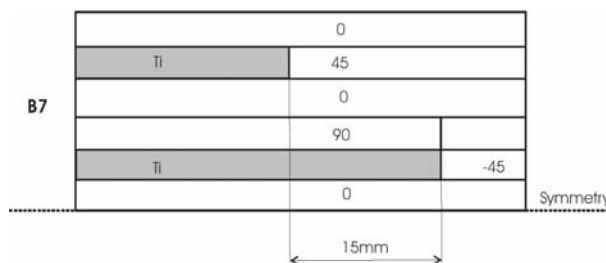


Figure 6: Geometry of the B7 specimen.

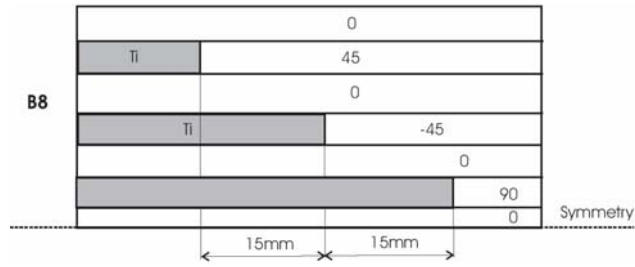


Figure 7: Geometry of the B8 specimen.

To simulate delamination, cohesive finite elements [11] are used along the Titanium-CFRP and CFRP-CFRP interfaces. In addition, cohesive finite elements are also placed in the elements that represent the 90° plies at the place where the titanium layers terminate (Figure 6). CPS4 plane stress elements are used to simulate all layers and 6 elements are used per ply thickness.

All the specimens were modelled making use of the symmetry along the through-thickness direction. An initial thermal step with  $\Delta T = -155\text{ }^{\circ}\text{C}$  was applied to simulate the curing process. After this step, the edges were constrained in the through-thickness direction, one end of the specimen was clamped, and a displacement was applied to the other end of the specimen. The models of the specimens B6 and B7 are 110mm long, 3mm thick and 15mm wide. The model of the specimen B8 has a thickness of 3.25mm and the other dimensions equal to those of the B6 and B7 specimens.

### 3.2.1 Model results

The analyses of the tensile specimens indicate that failure of the laminates occurs always due to fibre failure in a 0° ply, triggered by the stress concentration due to the debonding in the top (vertical) interface between titanium and the replaced ply or to crack propagation through a 90° ply. The baseline laminate without titanium was not simulated. A simple strength prediction based on the netting analysis predicts a failure stress of 925MPa for the baseline laminate. The numerically predicted strengths, taken as the ratio between the maximum load and the cross-section area of the specimens, are shown in Table 7 for the different specimens simulated.

Reference	Strength (MPa)
B6	610
B7	560
B8	758

Table 7: Predicted strengths.

The  $\sigma_{xx}$  stress field, plotted on the deformed shape at the failure load of each laminate, is shown in Figures 8 – 10.



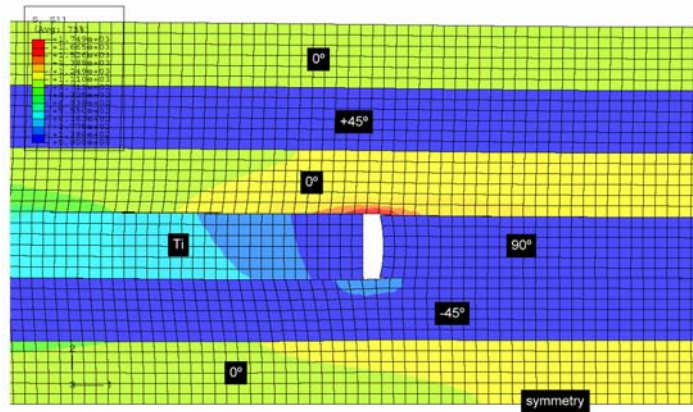


Figure 8: Deformed shape of the B6 specimen at the onset of fibre failure (ply 3, 610MPa).

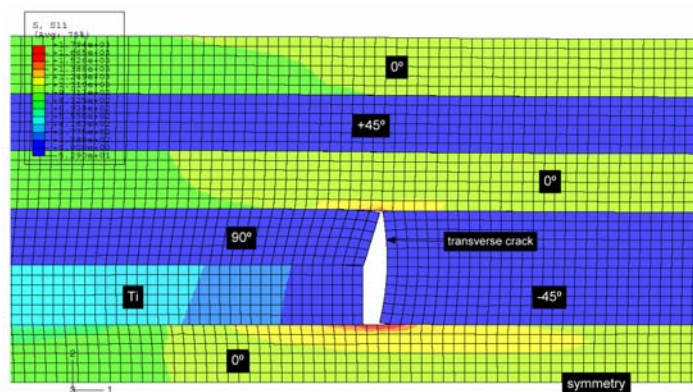


Figure 9: Deformed shape of the B7 specimen at the onset of fibre failure (ply 6, 560MPa).

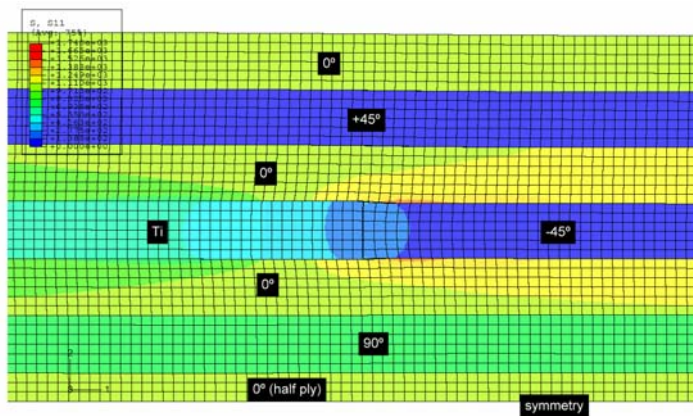


Figure 10: Deformed shape of the B8 specimen at the onset of fibre failure (ply 5, 758MPa).

#### 4. CONCLUSIONS

The numerical models of the bearing specimens indicate that:

- The bearing strength of the laminate increases when the titanium content is increased. There is a remarkable improvement of 158% when comparing the bearing strength of the B1 specimen (baseline configuration without titanium) with the one of the B8 specimen (with highest titanium content).

- Final failure occurs by the accumulation of fibre compressive damage. In addition, there is a small region of plastically deformed material in the titanium layer.

From the analysis of the results obtained in the simulation of the transition region, it is possible to conclude that:

- The specimen B8 shows the higher strength for the transition region (due to the high content of titanium and low content of 90° plies).
- The predicted strength of the transition region is always higher than the predicted strength of the bolt-bearing region. Therefore, the laminate fails as it should, in the bolt-bearing region and not in the transition region.

## ACKNOWLEDGEMENTS

The work presented in this paper has been funded by the European Space Agency (ESA) under the project 'Increase of Bolted Joint Performance'.

## REFERENCES

- 1- Fink, A. and Kolesnikov, B., "Hybrid titanium composite material improving composite structure coupling", *European Conference on Spacecraft Structures, Materials and Mechanical Testing*, Noordwijk, The Netherlands, 2005.
- 2- Fink, A., Camanho, P.P., Canay, M. and Obst, A., "Increase of bolted joint performance by means of local laminate hybridization", *First CEAS European Air and Space Conference*, Berlin, Germany, 2007.
- 3- Kolesnikov, B., Herbeck, L. and Fink, A. "CFRP/titanium hybrid material for improving composite bolted joints", *Composite Structures*, 2008; 83:368-380.
- 4- Camanho, P.P., "Application of numerical methods for the strength prediction of mechanically fastened joints in composite laminates", *PhD thesis*, Imperial College of Science, Technology and Medicine, London, 1999.
- 5- Abaqus 6.6 Users Manual, Dassault Systemes.
- 6- Hashin, Z., "Failure Criteria for Unidirectional Fiber Composites", *Journal of Applied Mechanics*, 1980; 47: 329-334.
- 7- Maimí, P., Camanho, P.P., Mayugo, J.A. and Dávila, C.G., "A continuum damage model for composite laminates: part I- constitutive model", *Mechanics of Materials*, 2007; 39: 897-908.
- 8- Maimí, P., Camanho, P.P., Mayugo, J.A. and Dávila, C.G., "A continuum damage model for composite laminates: part II- computational implementation and validation", *Mechanics of Materials*, 2007; 39: 909-919.
- 9- Camanho, P.P., Maimi, P. and Dávila, C.G., "Prediction of size effects in notched laminates using continuum damage mechanics", *Composites Science and Technology*, 2007; 67:2715-2727.
- 10- Xiao, Y. Wang, W.-X., Takao, Y. and Ishikawa, T., "The effective friction coefficient of a laminate composite, and analysis of pin-loaded plates", *Journal of Composite Materials*, 2000; 34:69-87.
- 11- Turon, A, Camanho, P.P., Costa, J. and Dávila, C.G., "A damage model for the simulation of delamination in advanced composites under variable-mode loading", *Mechanics of Materials*, 2006; 38:1072-1089.